

# True and spurious eigensolutions of elliptical membranes by using null-field boundary integral equations

Jia-Wei Lee<sup>1</sup>, Jeng-Tzong Chen<sup>1,2</sup> and Shyue-Yuh Leu<sup>3</sup>

<sup>1</sup>Department of Harbor and River Engineering,

National Taiwan Ocean University, Keelung, Taiwan

<sup>2</sup>Department of Mechanical and Mechatronic Engineering,

National Taiwan Ocean University, Keelung, Taiwan

<sup>3</sup>Department of Aviation Mechanical Engineering,

China University of Science and Technology, Hsinchu, Taiwan

M98520012@mail.ntou.edu.tw

**NSC PROJECT: NSC 98-2221-E-019-017-MY3**

## ABSTRACT

In this paper, the true and spurious eigensolutions of elliptical membranes appearing in boundary element method are examined by using the null-field boundary integral equation. To analytically study the eigenproblems with elliptical boundaries, the elliptic coordinates and Mathieu functions are adopted. The fundamental solutions are expanded into the degenerate kernel by using the elliptic coordinates and the boundary densities are expanded by using the eigenfunction expansion. The Jacobian terms may exist in the degenerate kernel, boundary density and boundary contour integration and they can cancel each other out. Therefore, the orthogonal relations are reserved in the boundary contour integral. It is interesting to find that if we only apply the real or the imaginary-part kernel to deal with a simply-connected elliptical membrane, spurious eigensolutions may appear. Even though we employ the complex-valued kernel, the spurious eigensolutions also occur in the case of a confocal elliptical annulus. Spurious eigenvalues depend on the geometry of inner boundary and the approach used. These two findings agree with those corresponding to the circular and annular cases, respectively. To verify the findings, the boundary element method is also implemented. Furthermore, the commercial finite-element code ABAQUS is also utilized to provide eigensolutions for comparisons. It is found that good agreement is obtained.

**Keywords:** eigensolutions, null-field boundary integral equation, elliptic coordinates, Mathieu functions, Jacobian, degenerate kernel.

## 1. INTRODUCTION

Eigenanalysis is very important for vibration and acoustics, because it can provide the fundamental information. In the recent years, many numerical methods

were utilized to determine eigenvalues and eigenmodes such as the finite element method (FEM) or the boundary element method (BEM). Although the FEM is a popular method, it needs to generate the mesh over the whole domain. The BEM only generate the mesh on the boundary but it may face with the calculation of the principal value and the pollution of spurious eigenvalues while dealing with the simply-connected problems only using the real or the imaginary-part kernel [1, 2, 3]. Even though we employ the complex-valued kernel for the multiply-connected eigenproblems, the spurious eigensolutions also occur [4, 5].

Recently, Chen *et al.* [6] applied the null-field boundary integral equation method (BIEM) in conjunction with the degenerate kernel and the Fourier series to solve the eigenproblems with circular boundaries. The advantage of free of calculating principal value is gained. This approach is one kind of semi-analytical and meshless methods. Spurious eigenvalues appear for the multiply-connected problems since the integral equation is used. Chen *et al.* [4, 5] pointed out that the spurious eigenvalues depend on the inner boundary with an illustrated annulus case.

However, all the previous examples [4, 5, 6] were focused on circular boundaries. Accordingly, we aim to extend this approach to deal with eigenproblems with elliptical boundaries. Regarding eigenproblems with elliptical boundaries, Troesch and Troesch [7] used the separation of variables to obtain the eigenfrequencies and nodal patterns of an elliptic membrane. Hong and Kim [8] also employed the separation of variables to determine the natural mode of hollow and elliptical annulus for cylindrical cavities. Both the elliptic coordinates and the Mathieu functions were used in the previous investigations [7, 8].

Following the successful experiences of employing the null-field BIEM to solve Laplace problems with elliptical boundaries [9], we extend the null-field BIEM

to study the spurious eigenvalue in BEM for eigenproblems with elliptical boundaries. The null-field BIEM is utilized in conjunction with the degenerate kernel and the eigenfunction expansion. To fully utilize the elliptical geometry for an analytical study, the elliptic coordinates and Mathieu functions [10] are used. The fundamental solution is expanded to the degenerate kernel by using the elliptic coordinates [11]. Also, the boundary densities are expanded by using the eigenfunction expansion in conjunction with a Jacobian term. The advantage of free of calculating principal value is gained. Finally, the true and spurious eigensolutions of an elliptical membrane and a confocal elliptical annulus are analytically derived by using the null-field BIEM and numerically verified by using the BEM and FEM, respectively.

## 2. PROBLEM STATEMENT AND THE PRESENT APPROACH

### 2.1 Problem statement

The governing equation for free vibration of a membrane is the Helmholtz equation as follows,

$$(\nabla^2 + k^2)u(\mathbf{x}) = 0, \quad \mathbf{x} \in D, \quad (1)$$

where  $\nabla^2$  is the Laplacian operator,  $k$  is the wave number,  $u(\mathbf{x})$  is the displacement,  $\mathbf{x}$  are the domain points and  $D$  is the domain of interest.

### 2.2 Dual boundary integral formulations — the conventional version

Based on the Green's third identity, the dual boundary integral equations for the domain point are shown below:

$$2\pi u(\mathbf{x}) = \int_B T(\mathbf{s}, \mathbf{x})u(\mathbf{s})dB(\mathbf{s}) - \int_B U(\mathbf{s}, \mathbf{x})t(\mathbf{s})dB(\mathbf{s}), \quad \mathbf{x} \in D, \quad (2)$$

$$2\pi t(\mathbf{x}) = \int_B M(\mathbf{s}, \mathbf{x})u(\mathbf{s})dB(\mathbf{s}) - \int_B L(\mathbf{s}, \mathbf{x})t(\mathbf{s})dB(\mathbf{s}), \quad \mathbf{x} \in D, \quad (3)$$

where  $\mathbf{s}$  are the source points,  $B$  is the boundary of membrane,  $t$  is the normal derivative of displacement and  $U(\mathbf{s}, \mathbf{x})$  is the fundamental function which satisfies

$$(\nabla^2 + k^2)U(\mathbf{s}, \mathbf{x}) = 2\pi\delta(\mathbf{x} - \mathbf{s}), \quad (4)$$

where  $\delta$  is the Dirac-delta function. The other kernel functions  $T(\mathbf{s}, \mathbf{x})$ ,  $L(\mathbf{s}, \mathbf{x})$  and  $M(\mathbf{s}, \mathbf{x})$  are defined by

$$T(\mathbf{s}, \mathbf{x}) = \frac{\partial U(\mathbf{s}, \mathbf{x})}{\partial n_s}, \quad (5)$$

$$L(\mathbf{s}, \mathbf{x}) = \frac{\partial U(\mathbf{s}, \mathbf{x})}{\partial n_x}, \quad (6)$$

$$M(\mathbf{s}, \mathbf{x}) = \frac{\partial^2 U(\mathbf{s}, \mathbf{x})}{\partial n_s \partial n_x}, \quad (7)$$

where  $n_x$  and  $n_s$  denote the unit outward normal vector at the field point and the source point, respectively.

By moving the field point  $\mathbf{x}$  to the boundary, the dual boundary integral equations for the boundary point can be obtained as follows:

$$\pi u(\mathbf{x}) = C.P.V \int_B T(\mathbf{s}, \mathbf{x})u(\mathbf{s})dB(\mathbf{s}) - R.P.V \int_B U(\mathbf{s}, \mathbf{x})t(\mathbf{s})dB(\mathbf{s}), \quad \mathbf{x} \in B, \quad (8)$$

$$\pi t(\mathbf{x}) = H.P.V \int_B M(\mathbf{s}, \mathbf{x})u(\mathbf{s})dB(\mathbf{s}) - C.P.V \int_B L(\mathbf{s}, \mathbf{x})t(\mathbf{s})dB(\mathbf{s}), \quad \mathbf{x} \in B, \quad (9)$$

where  $R.P.V.$ ,  $C.P.V.$  and  $H.P.V.$  denote the Riemann principal value (Riemann sum), Cauchy principal value and Hadamard (or so-called Mangler) principal value, respectively. By collocating the field point  $\mathbf{x}$  on the complementary domain, we obtain the dual null-field boundary integral equations as shown below:

$$0 = \int_B T(\mathbf{s}, \mathbf{x})u(\mathbf{s})dB(\mathbf{s}) - \int_B U(\mathbf{s}, \mathbf{x})t(\mathbf{s})dB(\mathbf{s}), \quad \mathbf{x} \in D^c, \quad (10)$$

$$0 = \int_B M(\mathbf{s}, \mathbf{x})u(\mathbf{s})dB(\mathbf{s}) - \int_B L(\mathbf{s}, \mathbf{x})t(\mathbf{s})dB(\mathbf{s}), \quad \mathbf{x} \in D^c, \quad (11)$$

where  $D^c$  denote the complementary domain.

### 2.3 Dual null-field boundary integral formulations — the present version

By introducing the degenerate kernels, the collocation point in Eqs. (2), (3), (10) and (11) can be located on the real boundary free of calculating principal value. Therefore, the dual boundary and dual null-field boundary integral equations can be rewritten in two parts as given in the following formulation of Eqs. (12) and (14), instead of three parts using Eqs. (2), (8) and (10) in the conventional BEM

$$2\pi u(\mathbf{x}) = \int_B T(\mathbf{s}, \mathbf{x})u(\mathbf{s})dB(\mathbf{s}) - \int_B U(\mathbf{s}, \mathbf{x})t(\mathbf{s})dB(\mathbf{s}), \quad \mathbf{x} \in D \cup B, \quad (12)$$

$$2\pi t(\mathbf{x}) = \int_B M(\mathbf{s}, \mathbf{x})u(\mathbf{s})dB(\mathbf{s}) - \int_B L(\mathbf{s}, \mathbf{x})t(\mathbf{s})dB(\mathbf{s}), \quad \mathbf{x} \in D \cup B, \quad (13)$$

and

$$0 = \int_B T(\mathbf{s}, \mathbf{x})u(\mathbf{s})dB(\mathbf{s}) - \int_B U(\mathbf{s}, \mathbf{x})t(\mathbf{s})dB(\mathbf{s}), \quad \mathbf{x} \in D^c \cup B, \quad (14)$$

$$0 = \int_B M(\mathbf{s}, \mathbf{x})u(\mathbf{s})dB(\mathbf{s}) - \int_B L(\mathbf{s}, \mathbf{x})t(\mathbf{s})dB(\mathbf{s}), \quad \mathbf{x} \in D^c \cup B. \quad (15)$$

It is found that Eqs. (12)-(15) can contain the boundary point ( $\mathbf{x} \rightarrow B$ ) since the kernel functions are expressed in terms of degenerate kernel.

### 2.4 Expansions of fundamental solution and boundary density using the elliptic coordinates

The closed-form fundamental solution as previously mentioned is

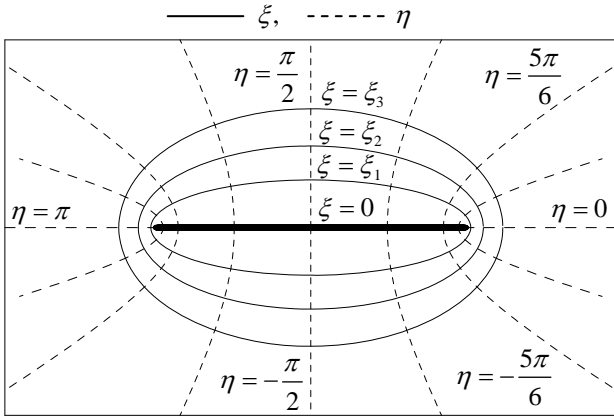


Figure 1 Elliptic coordinates.

$$U(\mathbf{s}, \mathbf{x}) = -\frac{i\pi H_0^{(1)}(kr)}{2}, \quad (16)$$

where  $r \equiv |\mathbf{s} - \mathbf{x}|$  is the distance between the source point and the field point,  $i$  is the imaginary number with  $i^2 = -1$  and  $H_0^{(1)}$  is the zeroth-order Hankel function of the first kind.

#### 2.4.1 Elliptic coordinates and Mathieu function

An elliptical membrane is considered in this work. In order to analytically study the problem with an elliptic boundary, the elliptic coordinates are used as shown in Fig. 1. The relation between the Cartesian coordinates  $(x, y)$  and the elliptic coordinates  $(\xi, \eta)$  is linked by

$$x = c \cosh(\xi) \cos(\eta), \quad y = c \sinh(\xi) \sin(\eta), \quad (17)$$

where the parameter  $c$  is the half distance between two foci, the coordinates  $\xi$  and  $\eta$  are the radial and angular coordinates, respectively. The ranges of two coordinates are  $\xi \geq 0$  and  $-\pi < \eta \leq \pi$ , respectively. It follows that the curves  $\xi = \text{constant}$  are a family of ellipses with two foci  $(\pm c, 0)$  and the curves  $\eta = \text{constant}$  are a family of hyperbolas with the same foci as shown in Fig. 1. In the elliptic coordinate system, the elliptic boundary is represented by  $\xi = \xi_1$  and its eccentricity is defined by

$$e = \text{sech}(\xi_1) = \sqrt{1 - (b/a)^2}, \quad (18)$$

where  $a$  and  $b$  are the half lengths of major and minor axes of the ellipse and can be described by

$$a = c \cosh(\xi_1), \quad (19)$$

$$b = c \sinh(\xi_1), \quad (20)$$

respectively and  $c$  can be determined by using the half lengths of major and minor axes as shown below:

$$c = \sqrt{a^2 - b^2}. \quad (21)$$

In the elliptic coordinates, the Eq.(1) is transformed to

$$\frac{1}{c^2 (\sinh^2(\xi) + \sin^2(\eta))} \left( \frac{\partial^2 u(\mathbf{x})}{\partial \xi^2} + \frac{\partial^2 u(\mathbf{x})}{\partial \eta^2} \right) + k^2 u(\mathbf{x}) = 0. \quad (22)$$

By using the method of separation of variables, the

displacement field  $u(\mathbf{x})$  can be assumed as

$$u(\mathbf{x}) = A(\eta)B(\xi). \quad (23)$$

Substituting the Eq.(23) to Eq.(22) and rearranging the terms, we have

$$\frac{d^2 A(\eta)}{d\eta^2} + (\sigma - 2q \cos(2\eta))A(\eta) = 0, \quad (24)$$

$$\frac{d^2 B(\xi)}{d\xi^2} - (\sigma - 2q \cosh(2\xi))B(\xi) = 0, \quad (25)$$

where  $\sigma$  is an arbitrary separation constant and the parameter  $q$  is defined by

$$q = \left( \frac{ck}{2} \right)^2. \quad (26)$$

Equations (24) and (25) are the so-called Mathieu and modified Mathieu equations, respectively. The solutions of Eqs. (24) and (25) are shown below:

$$A(\eta) = \begin{cases} Se_m(q, \eta), & m = 0, 1, \dots, \\ So_m(q, \eta), & m = 1, 2, \dots, \end{cases} \quad (27)$$

and

$$B(\xi) = \begin{cases} \alpha_m Je_m(q, \xi) + \beta_m Ye_m(q, \xi), & m = 0, 1, \dots, \\ \bar{\alpha}_m Jo_m(q, \xi) + \bar{\beta}_m Yo_m(q, \xi), & m = 1, 2, \dots, \end{cases} \quad (28)$$

respectively, where  $Se_m$  and  $So_m$  are the  $m$ th-order even and odd Mathieu functions (angular Mathieu functions) of the  $m$ th-order, respectively,  $Je_m$  and  $Jo_m$  are the  $m$ th-order even and odd modified Mathieu functions (radial Mathieu functions) of the first kind, respectively,  $Ye_m$  and  $Yo_m$  are the  $m$ th-order even and odd the modified Mathieu functions of the second kind, respectively,  $\alpha_m$ ,  $\beta_m$ ,  $\bar{\alpha}_m$ , and  $\bar{\beta}_m$  are the unknown coefficients. The normal derivative on the boundary point in the elliptic coordinates is defined by

$$t(\mathbf{x}) = \frac{\partial u(\mathbf{x})}{\partial n_x} = \frac{1}{J_x} \frac{\partial u(\mathbf{x})}{\partial \xi}, \quad \mathbf{x} \in B, \quad (29)$$

where  $J_x$  is the Jacobian term of the field point  $\mathbf{x}$  as shown below:

$$J_x = c \sqrt{(\sinh(\xi) \cos(\eta))^2 + (\cosh(\xi) \sin(\eta))^2}. \quad (30)$$

#### 2.4.2 Degenerate (separable) kernel for the fundamental solution using the elliptic coordinates

To fully utilize the property of elliptic geometry, the degenerate (separable or finite-rank) kernel and eigenfunction expansion are utilized for the analytical integration of boundary integrals. In the elliptic coordinates, the field point  $\mathbf{x}$  and source point  $\mathbf{s}$  can be expressed as  $\mathbf{x} = (\xi, \eta)$  and  $\mathbf{s} = (\xi_s, \eta_s)$ , respectively. By employing the addition theorem [10] for separating the source point and field point, the kernel functions,  $U(\mathbf{s}, \mathbf{x})$ ,  $T(\mathbf{s}, \mathbf{x})$ ,  $L(\mathbf{s}, \mathbf{x})$  and  $M(\mathbf{s}, \mathbf{x})$  are expanded in terms of degenerate kernel as shown below [11]:

$$U(\mathbf{s}, \mathbf{x}) = \begin{cases} -2\pi i \left( \sum_{m=0}^{\infty} \left[ \frac{Se_m(q, \eta_s)}{M_m^e(q)} \right] Se_m(q, \eta) Je_m(q, \xi_s) He_m(q, \xi) + \sum_{m=1}^{\infty} \left[ \frac{So_m(q, \eta_s)}{M_m^o(q)} \right] So_m(q, \eta) Jo_m(q, \xi_s) Ho_m(q, \xi) \right), & \xi \geq \xi_s \\ -2\pi i \left( \sum_{m=0}^{\infty} \left[ \frac{Se_m(q, \eta_s)}{M_m^e(q)} \right] Se_m(q, \eta) Je_m(q, \xi) He_m(q, \xi_s) + \sum_{m=1}^{\infty} \left[ \frac{So_m(q, \eta_s)}{M_m^o(q)} \right] So_m(q, \eta) Jo_m(q, \xi) Ho_m(q, \xi_s) \right), & \xi < \xi_s \end{cases}, \quad (31)$$

$$T(\mathbf{s}, \mathbf{x}) = \begin{cases} -2\pi i \frac{1}{J_s} \left( \sum_{m=0}^{\infty} \left[ \frac{Se_m(q, \eta_s)}{M_m^e(q)} \right] Se_m(q, \eta) Je'_m(q, \xi_s) He_m(q, \xi) + \sum_{m=1}^{\infty} \left[ \frac{So_m(q, \eta_s)}{M_m^o(q)} \right] So_m(q, \eta) Jo'_m(q, \xi_s) Ho_m(q, \xi) \right), & \xi > \xi_s \\ -2\pi i \frac{1}{J_s} \left( \sum_{m=0}^{\infty} \left[ \frac{Se_m(q, \eta_s)}{M_m^e(q)} \right] Se_m(q, \eta) Je_m(q, \xi) He'_m(q, \xi_s) + \sum_{m=1}^{\infty} \left[ \frac{So_m(q, \eta_s)}{M_m^o(q)} \right] So_m(q, \eta) Jo_m(q, \xi) Ho'_m(q, \xi_s) \right), & \xi < \xi_s \end{cases}, \quad (32)$$

$$L(\mathbf{s}, \mathbf{x}) = \begin{cases} -2\pi i \frac{1}{J_x} \left( \sum_{m=0}^{\infty} \left[ \frac{Se_m(q, \eta_s)}{M_m^e(q)} \right] Se_m(q, \eta) Je_m(q, \xi_s) He'_m(q, \xi) + \sum_{m=1}^{\infty} \left[ \frac{So_m(q, \eta_s)}{M_m^o(q)} \right] So_m(q, \eta) Jo_m(q, \xi_s) Ho'_m(q, \xi) \right), & \xi > \xi_s \\ -2\pi i \frac{1}{J_x} \left( \sum_{m=0}^{\infty} \left[ \frac{Se_m(q, \eta_s)}{M_m^e(q)} \right] Se_m(q, \eta) Je'_m(q, \xi) He_m(q, \xi_s) + \sum_{m=1}^{\infty} \left[ \frac{So_m(q, \eta_s)}{M_m^o(q)} \right] So_m(q, \eta) Jo'_m(q, \xi) Ho_m(q, \xi_s) \right), & \xi < \xi_s \end{cases}, \quad (33)$$

$$M(\mathbf{s}, \mathbf{x}) = \begin{cases} -2\pi i \frac{1}{J_s J_x} \left( \sum_{m=0}^{\infty} \left[ \frac{Se_m(q, \eta_s)}{M_m^e(q)} \right] Se_m(q, \eta) Je'_m(q, \xi_s) He'_m(q, \xi) + \sum_{m=1}^{\infty} \left[ \frac{So_m(q, \eta_s)}{M_m^o(q)} \right] So_m(q, \eta) Jo'_m(q, \xi_s) Ho'_m(q, \xi) \right), & \xi \geq \xi_s \\ -2\pi i \frac{1}{J_s J_x} \left( \sum_{m=0}^{\infty} \left[ \frac{Se_m(q, \eta_s)}{M_m^e(q)} \right] Se_m(q, \eta) Je'_m(q, \xi) He'_m(q, \xi_s) + \sum_{m=1}^{\infty} \left[ \frac{So_m(q, \eta_s)}{M_m^o(q)} \right] So_m(q, \eta) Jo'_m(q, \xi) Ho'_m(q, \xi_s) \right), & \xi < \xi_s \end{cases}, \quad (34)$$

where  $J_s$  is the Jacobian term of the source point,  $\mathbf{s}$ , as shown below:

$$J_s = c \sqrt{(\sinh(\xi_s) \cos(\eta_s))^2 + (\cosh(\xi_s) \sin(\eta_s))^2}, \quad (35)$$

$He_m$  and  $Ho_m$  are the even and odd  $m$ th-order modified Mathieu functions (Mathieu-Hankel functions) of the third kind, respectively and are defined as

$$He_m(q, \xi) = Je_m(q, \xi) + iYe_m(q, \xi), \quad (36)$$

$$Ho_m(q, \xi) = Jo_m(q, \xi) + iYo_m(q, \xi), \quad (37)$$

$M_m^e$  and  $M_m^o$  are the normalized constants and can be obtained by

$$M_m^e(q) = \int_{-\pi}^{\pi} Se_m(q, \eta) Se_n(q, \eta) d\eta = \begin{cases} \pi, & m = n, \\ 0, & m \neq n, \end{cases} \quad (38)$$

$$M_m^o(q) = \int_{-\pi}^{\pi} So_m(q, \eta) So_n(q, \eta) d\eta = \begin{cases} \pi, & m = n, \\ 0, & m \neq n, \end{cases} \quad (39)$$

$$\int_{-\pi}^{\pi} Se_m(q, \eta) So_n(q, \eta) d\eta = 0. \quad (40)$$

Equations (38)-(40) are also called the orthogonal relations of the angular Mathieu functions. It is noted that  $U$  and  $M$  kernels in Eqs. (31) and (34) contain the equal sign of  $\xi = \xi_s$  while  $T$  and  $L$  kernels do not include the equal sign due to the discontinuity. The contour plots of the closed-form fundamental solution and the degenerate kernel by using Eqs. (16) and (31), respectively, are shown in Table 1.

#### 2.4.3 Eigenfunction expansion for unknown boundary densities

For the unknown boundary densities, we apply the eigenfunction expansion to approximate the displacement,

$u(\mathbf{s})$ , and its normal derivative,  $t(\mathbf{s}) = \frac{1}{J_s} \frac{\partial u(\mathbf{s})}{\partial \xi_s}$  along

the elliptic boundary as

$$u(\mathbf{s}) = \sum_{n=0}^{\infty} g_n Se_n(q, \eta_s) + \sum_{n=1}^{\infty} h_n So_n(q, \eta_s), \quad \mathbf{s} \in B, \quad (41)$$

$$t(\mathbf{s}) = \frac{1}{J_s} \left( \sum_{n=0}^{\infty} p_n Se_n(q, \eta_s) + \sum_{n=1}^{\infty} q_n So_n(q, \eta_s) \right), \quad \mathbf{s} \in B, \quad (42)$$

respectively, where  $g_n$ ,  $h_n$ ,  $p_n$  and  $q_n$  are the unknown coefficients of the eigenfunctions. The Jacobian term  $J_s$  may occur in the kernels of Eqs. (32)-(34), boundary densities of the Eq. (42) and boundary contour integration ( $dB(\mathbf{s}) = J_s d\eta_s$ ). However, the Jacobian terms can be cancelled each other out and the orthogonal relations can be fully utilized in the boundary integration.

### 3. ANALYTICAL STUDY ON TRUE AND SPURIOUS EIGENSOLUTION OF ELLIPTICAL MEMBRANES

#### 3.1 A simply-connected elliptical membrane

Now, we consider an elliptic membrane subject to the Dirichlet and Neumann B.C.s as shown in Fig. 2,

$$u(\mathbf{x}) = u(\xi_1, \eta) = 0, \quad (\text{Dirichlet B.C.}), \quad (43)$$

$$t(\mathbf{x}) = \frac{1}{J_x} \frac{\partial u(\xi, \eta)}{\partial \xi} \Big|_{\xi=\xi_1} = 0, \quad (\text{Neumann B.C.}), \quad (44)$$

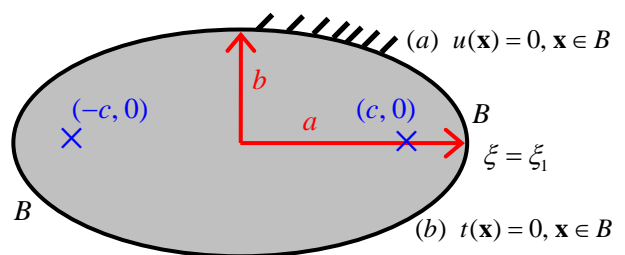


Figure 2 An elliptical membrane subject to the (a). Dirichlet and (b). Neumann B.C.s.

respectively, where  $\mathbf{x} \in B$ . The elliptical membrane is bounded by  $\xi = \xi_1$  as given below:

$$\xi_1 = \tanh^{-1}(b/a). \quad (45)$$

First, we employ Eq. (14) to derive the eigensolution. Substituting Eqs. (31) and (42) to the Eq. (14), and employing the orthogonal relations, we have

$$\begin{aligned} -2\pi i \left( \sum_{m=0}^{\infty} p_m S e_m(q, \eta) J e_m(q, \xi_1) H e_m(q, \xi_1) \right. \\ \left. + \sum_{m=1}^{\infty} q_m S o_m(q, \eta) J o_m(q, \xi_1) H o_m(q, \xi_1) \right) = 0, \end{aligned} \quad (46)$$

for the Dirichlet problem. Similarly, substitution of Eqs. (32) and (41) into Eq. (14) yields

$$\begin{aligned} -2\pi i \left( \sum_{m=0}^{\infty} g_m S e_m(q, \eta) J e'_m(q, \xi_1) H e_m(q, \xi_1) \right. \\ \left. + \sum_{m=1}^{\infty} h_m S o_m(q, \eta) J o'_m(q, \xi_1) H o_m(q, \xi_1) \right) = 0, \end{aligned} \quad (47)$$

for the Neumann problem. Since

$$\sum_{m=0}^{\infty} (p_m)^2 + \sum_{m=1}^{\infty} (q_m)^2 = 0 \quad \text{in Eq. (46) and}$$

$$\sum_{m=0}^{\infty} (g_m)^2 + \sum_{m=1}^{\infty} (h_m)^2 = 0 \quad \text{in Eq. (47) imply a trivial}$$

solution, we obtain only the true eigenequations as shown below:

$$J e_m(q, \xi_1) = 0, \quad (48)$$

$$J o_m(q, \xi_1) = 0, \quad (49)$$

for the Dirichlet problem and

$$J e'_m(q, \xi_1) = 0, \quad (50)$$

$$J o'_m(q, \xi_1) = 0, \quad (51)$$

for the Neumann problem. Similarly, the eigensolutions can be obtained by using the Eq. (15) as given below:

$$\begin{aligned} \frac{-2\pi i}{J_{\mathbf{x}}} \left( \sum_{m=0}^{\infty} p_m S e_m(q, \eta) J e_m(q, \xi_1) H e'_m(q, \xi_1) \right. \\ \left. + \sum_{m=1}^{\infty} q_m S o_m(q, \eta) J o_m(q, \xi_1) H o'_m(q, \xi_1) \right) = 0, \end{aligned} \quad (52)$$

for the Dirichlet problem and

$$\begin{aligned} \frac{-2\pi i}{J_{\mathbf{x}}} \left( \sum_{m=0}^{\infty} g_m S e_m(q, \eta) J e'_m(q, \xi_1) H e'_m(q, \xi_1) \right. \\ \left. + \sum_{m=1}^{\infty} h_m S o_m(q, \eta) J o'_m(q, \xi_1) H o'_m(q, \xi_1) \right) = 0, \end{aligned} \quad (53)$$

for the Neumann problem. By employ the hypersingular formulation of Eq. (15), we also obtain the same true eigenequation of Eqs. (48)-(51). Since we employ the complex-valued BIEM, no spurious eigensolutions appear for the simply-connected problem. If we only apply the real or the imaginary-part kernel alone, spurious eigensolutions occur and the results are shown in Table 2.

### 3.2 An elliptical annulus

Following successful experiences in annular membranes [4, 5], it has been revealed that the corresponding mechanism of the spurious eigensolutions

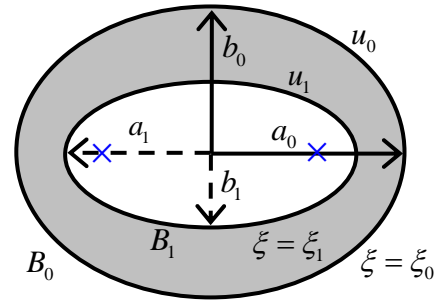


Figure 3 Sketch of a confocal elliptical annulus.

of the multiply-connected problem depends on the geometry of inner boundary and the approach used. Now, we extend to study elliptical cases by using Eqs. (14) and (15) in conjunction with the elliptic coordinates and the Mathieu functions. An elliptical annulus is considered as shown in Fig. 3. In order to analytically formulate the problem, the same half distance between two foci is used, i.e., the parameters of the confocal ellipse are  $\xi = \xi_0$  and  $\xi = \xi_1$  for outer and inner boundaries, respectively. The confocal membrane is subject to fixed-fixed BC as shown below:

$$u(\mathbf{x}) = 0, \quad \mathbf{x} \in B_0 \cup B_1. \quad (54)$$

Equations. (14) and (15) are written as

$$0 = \sum_{j=0}^1 \int_{B_j} T(\mathbf{s}_j, x) u(\mathbf{s}_j) dB(\mathbf{s}_j) \quad (55)$$

$$- \sum_{j=0}^1 \int_{B_j} U(\mathbf{s}_j, x) t(\mathbf{s}_j) dB(\mathbf{s}_j), \quad \mathbf{x} \in D^c \cup B,$$

$$0 = \sum_{j=0}^1 \int_{B_j} M(\mathbf{s}_j, x) u(\mathbf{s}_j) dB(\mathbf{s}_j) \quad (56)$$

$$- \sum_{j=0}^1 \int_{B_j} L(\mathbf{s}_j, x) t(\mathbf{s}_j) dB(\mathbf{s}_j), \quad \mathbf{x} \in D^c \cup B,$$

and boundary densities are expressed by

$$t_0(\mathbf{s}) = \frac{1}{J_{\mathbf{s}}} \left( \sum_{n=0}^{\infty} p_n^0 S e_n(q, \eta_s) + \sum_{n=1}^{\infty} q_n^0 S o_n(q, \eta_s) \right), \quad \mathbf{s} \in B_0, \quad (57)$$

$$t_1(\mathbf{s}) = \frac{1}{J_{\mathbf{s}}} \left( \sum_{n=0}^{\infty} p_n^1 S e_n(q, \eta_s) + \sum_{n=1}^{\infty} q_n^1 S o_n(q, \eta_s) \right), \quad \mathbf{s} \in B_1, \quad (58)$$

where  $p_n^j$  and  $q_n^j$  are the unknown coefficients of the eigenfunctions on  $B_j$  ( $j = 0, 1$ ). Substituting Eqs. (57), (58) and (31) to Eq. (55) and collocating the field point exactly on the outer boundary, we have

$$\begin{aligned} -2\pi i \left( \sum_{m=0}^{\infty} p_m^0 S e_m(q, \eta) J e_m(q, \xi_0) H e_m(q, \xi_0) \right. \\ \left. + \sum_{m=1}^{\infty} q_m^0 S o_m(q, \eta) J o_m(q, \xi_0) H o_m(q, \xi_0) \right. \\ \left. + \sum_{m=0}^{\infty} p_m^1 S e_m(q, \eta) J e_m(q, \xi_1) H e_m(q, \xi_0) \right. \\ \left. + \sum_{m=1}^{\infty} q_m^1 S o_m(q, \eta) J o_m(q, \xi_1) H o_m(q, \xi_0) \right) = 0. \end{aligned} \quad (59)$$

By similarly collocating the field point of Eq. (55) exactly on the inner boundary, we have

$$\begin{aligned}
 & -2\pi i \left( \sum_{m=0}^{\infty} p_m^0 Se_m(q, \eta) Je_m(q, \xi_1) He_m(q, \xi_0) \right. \\
 & + \sum_{m=1}^{\infty} q_m^0 So_m(q, \eta) Jo_m(q, \xi_1) Ho_m(q, \xi_0) \\
 & + \sum_{m=0}^{\infty} p_m^1 Se_m(q, \eta) Je_m(q, \xi_1) He_m(q, \xi_1) \\
 & \left. + \sum_{m=1}^{\infty} q_m^1 So_m(q, \eta) Jo_m(q, \xi_1) Ho_m(q, \xi_1) \right) = 0.
 \end{aligned} \tag{60}$$

According to Eqs. (51) and (60), we obtain the relation between  $p_m^0$ ,  $q_m^0$  and  $p_m^1$ ,  $q_m^1$  as follows:

$$p_m^0 = -\frac{Je_m(q, \xi_1) He_m(q, \xi_0)}{Je_m(q, \xi_0) He_m(q, \xi_0)} p_m^1, m = 0, 1, 2 \dots \tag{61}$$

$$q_m^0 = -\frac{Jo_m(q, \xi_1) Ho_m(q, \xi_0)}{Jo_m(q, \xi_0) Ho_m(q, \xi_0)} q_m^1, m = 1, 2 \dots \tag{62}$$

and

$$p_m^0 = -\frac{Je_m(q, \xi_1) He_m(q, \xi_1)}{Je_m(q, \xi_1) He_m(q, \xi_0)} p_m^1, m = 0, 1, 2 \dots \tag{63}$$

$$q_m^0 = -\frac{Jo_m(q, \xi_1) Ho_m(q, \xi_1)}{Jo_m(q, \xi_1) Ho_m(q, \xi_0)} q_m^1, m = 1, 2 \dots, \tag{64}$$

respectively. Combination of Eqs. (61)-(64), we obtain four possible eigenequations,

$$\begin{aligned}
 & Je_m(q, \xi_0) Ye_m(q, \xi_1) \\
 & - Je_m(q, \xi_1) Ye_m(q, \xi_0) = 0, m = 0, 1, 2 \dots,
 \end{aligned} \tag{65}$$

$$\begin{aligned}
 & Jo_m(q, \xi_0) Yo_m(q, \xi_1) \\
 & - Jo_m(q, \xi_1) Yo_m(q, \xi_0) = 0, m = 1, 2 \dots,
 \end{aligned} \tag{66}$$

and

$$Je_m(q, \xi_1) = 0, m = 0, 1, 2 \dots, \tag{67}$$

$$Jo_m(q, \xi_1) = 0, m = 1, 2 \dots. \tag{68}$$

Based on Eq. (56), we similarly obtain four possible eigenequations,

$$Je'_m(q, \xi_1) = 0, m = 0, 1, 2 \dots, \tag{69}$$

$$Jo'_m(q, \xi_1) = 0, m = 1, 2 \dots, \tag{70}$$

and the other two are the same with Eqs. (65) and (66). If we employ two different approaches to solve the same problem, we should obtain the same true solution. Therefore, it indicates that Eqs. (67)-(68) and Eqs. (69)-(70) are the spurious eigenequations by using Eqs. (55) and (56), respectively. The true and spurious eigenequations for problems with various boundary conditions (free-fixed, fixed-free and free-free) are shown in Table 3. It is interesting to find that the spurious eigenequations depend on the geometry of inner boundary and the approach used. This conclusion agrees well with the annular case [4, 5].

#### 4. NUMERICAL EXAMPLES

In the following case studies, we consider an elliptic membrane and a confocal elliptical annulus in cases 1 and 2, respectively, subject to the Dirichlet boundary conditions. The eigensolutions obtained by using the analytical derivations, the BEM and the FEM are compared for validations. Note that, the second-order

acoustic elements AC2D8 of ABAQUS are applied to mesh the finite-element models.

#### Case 1. An elliptical membrane

In the first case, an elliptical membrane subject to the Dirichlet boundary condition is considered as shown in Fig. 2(a). The half lengths of major and eccentricity are  $a=1$  and  $e=\sqrt{0.75}$ , respectively. The results of the analytical derivations, BEM and FEM are shown in Tables 3 and 4, respectively. Imaginary-part BEM yields spurious multiplicities in Table 3(c). Good agreement is made. True and spurious solutions are analytically classified and found numerically.

#### Case 2. A confocal elliptical annulus

In this case, a confocal ellipse is considered. The outer and inner boundary conditions are both Dirichlet types. The half lengths of major and eccentricity for the inner boundary are  $a_1=1$  and  $e_1=\sqrt{0.75}$ , respectively. The parameter  $\xi$  of inner boundary is  $\xi_1 = \tanh^{-1}(b_1/a_1)$  and the outer boundary is described by  $\xi_0 = 2\xi_1$ . The results of the analytical derivations, BEM and FEM are shown in Tables 5 and 6. Good agreement is made. True and spurious solutions are analytically predicted and numerically verified by using the BEM.

### 5. CONCLUSIONS

In this paper, we have successfully applied the null-field BIEM to deal with the eigenproblems with elliptical boundaries. True and spurious eigensolutions are analytically derived and numerically performed in the two examples. In a simply-connected case, the spurious eigenequations occur once we only employ the real-part or imag-part kernel alone in the null-field BIEM. Furthermore, the spurious eigenequations depend on the geometry of inner boundary in the doubly-connected domain and the approach used for the confocal case, even though the complex-valued BIEM is employed. These two findings are the same with those corresponding to the circle and the annular cases, respectively.

### 6. ACKNOWLEDGEMENT

Financial support from the National Science Council under Grant No. NSC-98-2221-E-019-017-MY3 for National Taiwan Ocean University is gratefully acknowledged.

### 7. REFERENCES

- [1] S. R. Kuo, J. T. Chen, and C. X. Huang, "Analytical study and numerical experiments for true and spurious eigensolutions of a circular cavity using the real-part dual BEM," *Int. J. Numer. Meth. Engng.*, vol. 48, pp. 1401-1422, 2000.
- [2] J. T. Chen, J. W. Lee and Y. C. Cheng, "On the spurious eigensolutions for the real-part boundary element method," *Engng. Anal. Bound. Elem.*, vol. 33,

pp. 342-355, 2009.

[3] J. T. Chen, S. Y. Lin, Y. T. Lee and I. L. Chen, "Analytical and numerical studies of free vibrations of plate by imaginary-part BEM formulations," *J. Sound Vib.*, vol. 293, pp. 380-408, 2006.

[4] J. T. Chen, J. H. Lin, S. R. Kuo and S. W. Chyuan, "Boundary element analysis for the Helmholtz eigenvalue problems with a multiply-connected domain," *Proc. R. Soc. Lond., Ser. A*, vol. 457, pp. 2521-2546, 2001.

[5] J. T. Chen, L. W. Liu and H. K. Hong, "Spurious and true eigensolutions of Helmholtz BIEs and BEMs for a multiply-connected problem," *Proc. R. Soc. Lond., Ser. A*, vol. 459, pp.1891-1925, 2003.

[6] J. T. Chen, C. T. Chen and I. L. Chen, "Null-field integral equation approach for eigenproblems with

circular boundaries," *J. Comp. Acoust.*, vol. 15, No. 4, pp. 401-428, 2007.

[7] B. A. Troesch and H. R. Troesch, "Eigenfrequencies of an elliptic membrane," *Math. Comp.*, vol. 27, No. 124, pp. 755-765, 1973.

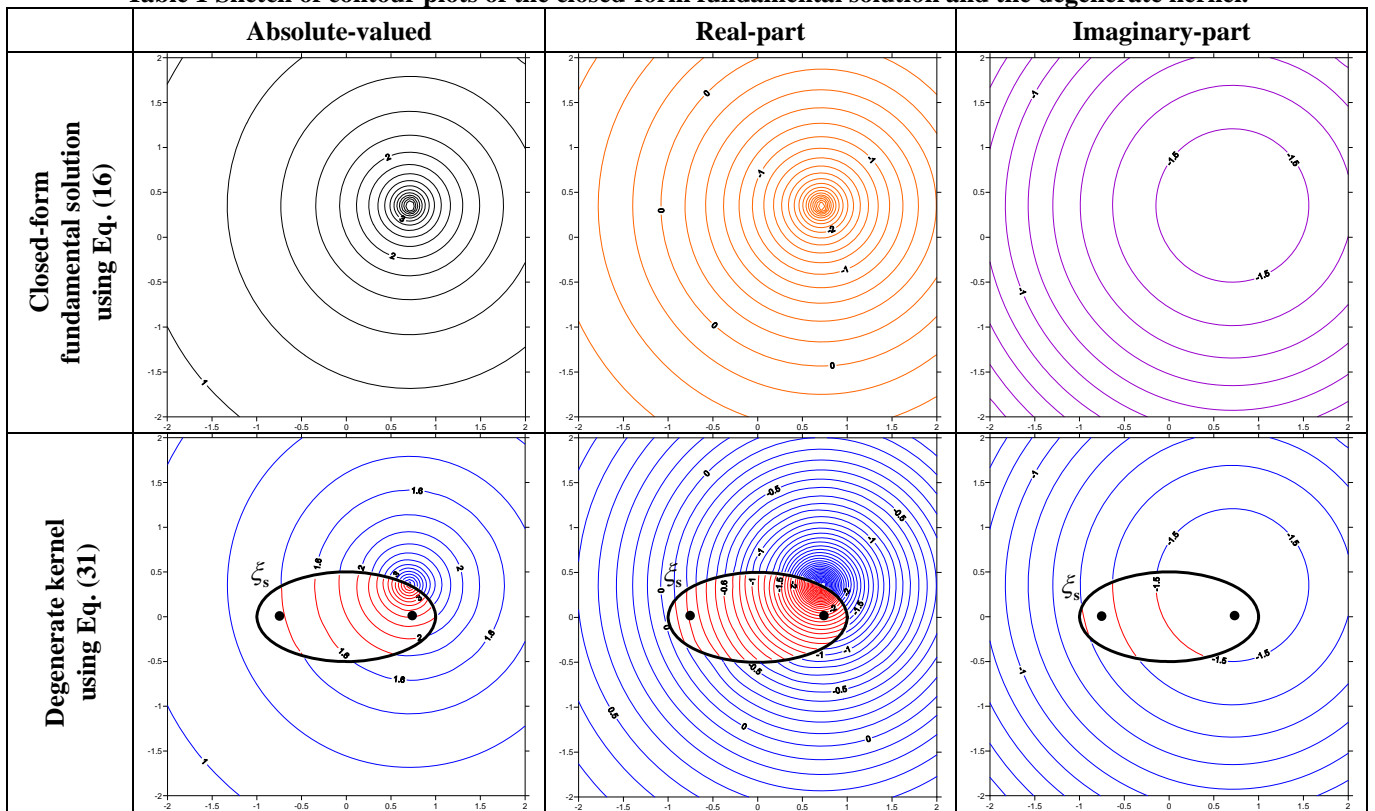
[8] K. Hong and J. Kim, "Natural mode analysis of hollow and annular elliptical cylindrical cavities," *J. Sound Vib.*, vol. 183, No. 2, pp. 327-351, 1995.

[9] Y. T. Lee, Applications of the addition theorem in engineering problems, Ph.D. Dissertation, National Taiwan Ocean University, Keelung, Taiwan, 2009.

[10] S. Zhang and J. Jin, *Computation of Special Functions*, John Wiley & Sons, New York, 1996.

[11] P. Morese and H. Feshbach, *Method of Theoretical Physics*, McGraw-Hill, New York, 1953.

**Table 1 Sketch of contour plots of the closed-form fundamental solution and the degenerate kernel.**

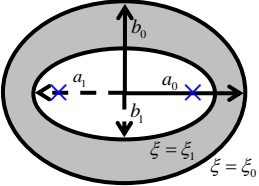
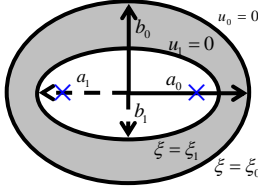
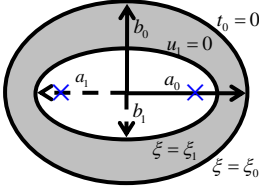
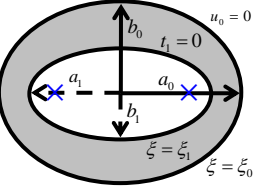
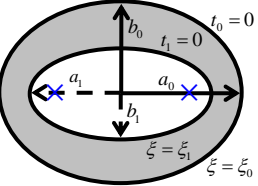
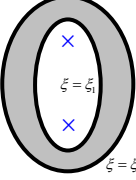
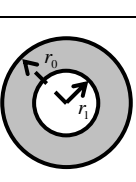
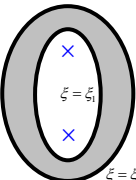
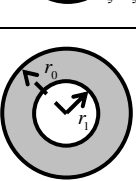
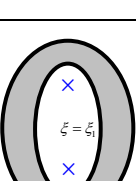
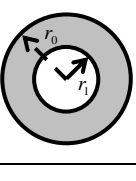
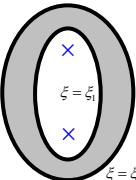
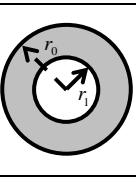


**Table 2 True and spurious eigenequations by using the real-part and imaginary-part BIEMs.**

	Dirichlet BC	Neumann BC
UT(real-part)	$\{J_{e_m}\}[Y_{e_m}] = 0$ or $\{J_{o_m}\}[Y_{o_m}] = 0$ $\{J_m\}[Y_m] = 0$ (circular case)	$\{J'_{e_m}\}[Y_{e_m}] = 0$ or $\{J'_{o_m}\}[Y_{o_m}] = 0$ $\{J'_m\}[Y_m] = 0$ (circular case)
LM(real-part)	$\{J_{e_m}\}[Y'_{e_m}] = 0$ or $\{J_{o_m}\}[Y'_{o_m}] = 0$ $\{J_m\}[Y'_m] = 0$ (circular case)	$\{J'_{e_m}\}[Y'_{e_m}] = 0$ or $\{J'_{o_m}\}[Y'_{o_m}] = 0$ $\{J'_m\}[Y'_m] = 0$ (circular case)
UT(imaginary-part)	$\{J_{e_m}\}[J_{e_m}] = 0$ or $\{J_{o_m}\}[J_{o_m}] = 0$ $\{J_m\}[J_m] = 0$ (circular case)	$\{J'_{e_m}\}[J_{e_m}] = 0$ or $\{J'_{o_m}\}[J_{o_m}] = 0$ $\{J'_m\}[J_m] = 0$ (circular case)
LM(imaginary-part)	$\{J_{e_m}\}[J'_{e_m}] = 0$ or $\{J_{o_m}\}[J'_{o_m}] = 0$ $\{J_m\}[J'_m] = 0$ (circular case)	$\{J'_{e_m}\}[J'_{e_m}] = 0$ or $\{J'_{o_m}\}[J'_{o_m}] = 0$ $\{J'_m\}[J'_m] = 0$ (circular case)

Notes: (a) the equation inside the brace and the square bracket denote the true and spurious eigenequation, respectively.  
 (b)  $J_{e_m}$  and  $Y_{e_m}$ ,  $m = 0, 1, 2 \dots$  and  $J_{o_m}$  and  $Y_{o_m}$ ,  $m = 1, 2 \dots$ .

**Table 3 True and spurious eigenequations for the confocal elliptical annulus subject to various boundary conditions.**

						
		<b>Figure sketch</b>	<b>(Fixed-fixed)</b>	<b>(Free-fixed)</b>	<b>(Fixed-free)</b>	<b>(Free-free)</b>
<b>UT equation using Eq. (14)</b>	<b>True eigenequation</b>		$Je_m(q, \xi_0)Ye_m(q, \xi_1)$ $-Je_m(q, \xi_1)Ye_m(q, \xi_0) = 0$	$Je'_m(q, \xi_0)Ye_m(q, \xi_1)$ $-Je_m(q, \xi_1)Ye'_m(q, \xi_0) = 0$	$Je_m(q, \xi_0)Ye'_m(q, \xi_1)$ $-Je'_m(q, \xi_1)Ye_m(q, \xi_0) = 0$	$Je'_m(q, \xi_0)Ye'_m(q, \xi_1)$ $-Je'_m(q, \xi_1)Ye'_m(q, \xi_0) = 0$
			$Jo_m(q, \xi_0)Yo_m(q, \xi_1)$ $-Jo_m(q, \xi_1)Yo_m(q, \xi_0) = 0$	$Jo'_m(q, \xi_0)Yo_m(q, \xi_1)$ $-Jo_m(q, \xi_1)Yo'_m(q, \xi_0) = 0$	$Jo_m(q, \xi_0)Yo'_m(q, \xi_1)$ $-Jo'_m(q, \xi_1)Yo_m(q, \xi_0) = 0$	$Jo'_m(q, \xi_0)Yo'_m(q, \xi_1)$ $-Jo'_m(q, \xi_1)Yo'_m(q, \xi_0) = 0$
	<b>Spurious eigenequation</b>		$Je_m(q, \xi_1) = 0$	$Je_m(q, \xi_1) = 0$	$Je_m(q, \xi_1) = 0$	$Je_m(q, \xi_1) = 0$
			$Jo_m(q, \xi_1) = 0$	$Jo_m(q, \xi_1) = 0$	$Jo_m(q, \xi_1) = 0$	$Jo_m(q, \xi_1) = 0$
			$J_m(kr_1) = 0$ (annular case)	$J_m(kr_1) = 0$ (annular case)	$J_m(kr_1) = 0$ (annular case)	$J_m(kr_1) = 0$ (annular case)
	<b>LM equation using Eq. (15)</b>	<b>True eigenequation</b>		$Je_m(q, \xi_0)Ye_m(q, \xi_1)$ $-Je_m(q, \xi_1)Ye_m(q, \xi_0) = 0$	$Je'_m(q, \xi_0)Ye_m(q, \xi_1)$ $-Je_m(q, \xi_1)Ye'_m(q, \xi_0) = 0$	$Je_m(q, \xi_0)Ye'_m(q, \xi_1)$ $-Je'_m(q, \xi_1)Ye_m(q, \xi_0) = 0$
			$Jo_m(q, \xi_0)Yo_m(q, \xi_1)$ $-Jo_m(q, \xi_1)Yo_m(q, \xi_0) = 0$	$Jo'_m(q, \xi_0)Yo_m(q, \xi_1)$ $-Jo_m(q, \xi_1)Yo'_m(q, \xi_0) = 0$	$Jo_m(q, \xi_0)Yo'_m(q, \xi_1)$ $-Jo'_m(q, \xi_1)Yo_m(q, \xi_0) = 0$	$Jo'_m(q, \xi_0)Yo'_m(q, \xi_1)$ $-Jo'_m(q, \xi_1)Yo'_m(q, \xi_0) = 0$
<b>Spurious eigenequation</b>			$Je'_m(q, \xi_1) = 0$	$Je'_m(q, \xi_1) = 0$	$Je'_m(q, \xi_1) = 0$	$Je'_m(q, \xi_1) = 0$
			$Jo'_m(q, \xi_1) = 0$	$Jo'_m(q, \xi_1) = 0$	$Jo'_m(q, \xi_1) = 0$	$Jo'_m(q, \xi_1) = 0$
			$J'_m(kr_1) = 0$ (annular case)	$J'_m(kr_1) = 0$ (annular case)	$J'_m(kr_1) = 0$ (annular case)	$J'_m(kr_1) = 0$ (annular case)

**Table 3(a) The former ten eigenvalues of an elliptical membrane subject to the Dirichlet boundary condition by using the complex-valued kernel.**

Method \ Eigenvalue	$k_1$	$k_2$	$k_3$	$k_4$	$k_5$	$k_6$	$k_7$	$k_8$	$k_9$	$k_{10}$
Present method	3.777	5.010	6.334	6.852	7.714	7.981	9.132	9.170	9.977	10.408
Complex-valued BEM (No. elements=30)	3.795	5.031	6.359	6.881	7.744	8.010	9.164	9.196	10.019	10.430
ABQUAS (No. elements=774)	3.777	5.010	6.333	6.852	7.714	7.981	9.132	9.170	9.977	10.408

**Table 3(b) The former ten eigenvalues of an elliptical membrane subject to the Dirichlet boundary condition by using the real-part kernel.**

Method \ Eigenvalue	$k_1$	$k_2$	$k_3$	$k_4$	$k_5$	$k_6$	$k_7$	$k_8$	$k_9$	$k_{10}$
Present method	(1.220)	(2.610)	(3.756)	3.777	(4.033)	(4.938)	5.010	(5.471)	(6.187)	6.334
Real-part BEM (No. elements=30)	(1.225)	(2.622)	(3.774)	3.795	(4.052)	(4.963)	5.032	(5.498)	(6.221)	6.360

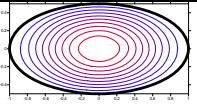
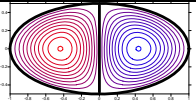
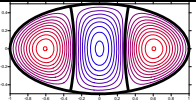
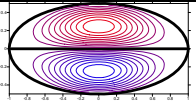
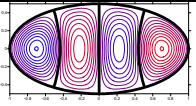
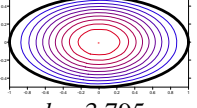
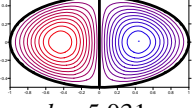
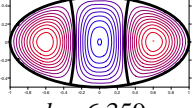
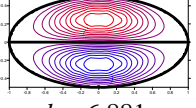
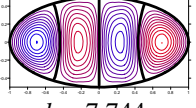
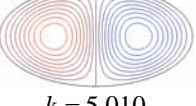
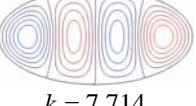
Note: the data inside parentheses denote the spurious eigenvalue.

**Table 3(c) The former five eigenvalues of an elliptical membrane subject to the Dirichlet boundary condition by using the imaginary-part kernel.**

Method \ Eigenvalue	$k_1$	$k_2$	$k_3$	$k_4$	$k_5$
Present method	3.777	5.010	6.334	6.852	7.714
Imag-part BEM (No. elements=12)	3.865 3.911*	5.128 5.186*	6.512	7.037	7.965

\* spurious multiplicity

**Table 4 The former five modes for an elliptical membrane.**

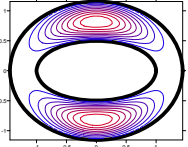
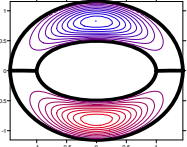
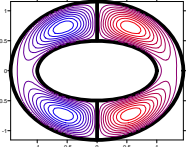
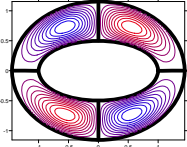
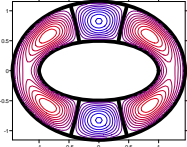
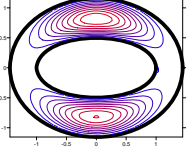
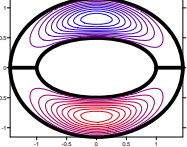
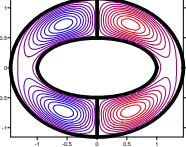
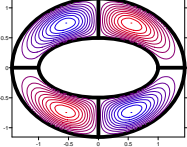
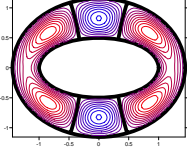
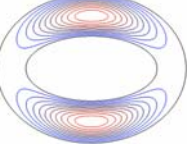
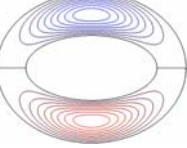
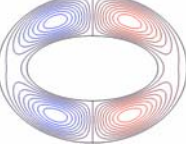
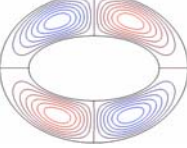
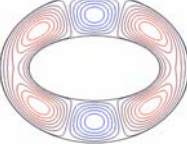
Method \ Eigenmode	mode 1	mode 2	mode 3	mode 4	mode 5
Present method	 $k = 3.777$	 $k = 5.010$	 $k = 6.334$	 $k = 6.852$	 $k = 7.714$
Complex-valued BEM (No. elements=30)	 $k = 3.795$	 $k = 5.031$	 $k = 6.359$	 $k = 6.881$	 $k = 7.744$
ABQUAS (No. elements=774)	 $k = 3.777$	 $k = 5.010$	 $k = 6.333$	 $k = 6.852$	 $k = 7.714$

**Table 5 The former ten eigenvalues for a confocal elliptical annulus.**

Method \ Eigenvalue	$k_1$	$k_2$	$k_3$	$k_4$	$k_5$	$k_6$	$k_7$	$k_8$	$k_9$	$k_{10}$
Present method	(3.777)	(5.010)	5.104	5.104	5.699	5.709	6.251	6.306	(6.334)	6.716
Complex-valued BEM (No. elements=100)	(3.783)	(5.018)	5.112	5.112	5.707	5.717	6.259	6.314	(6.343)	6.725
ABQUAS (No. elements=2460)	-	-	5.104	5.104	5.699	5.709	6.251	6.306	-	6.716

Note: the data inside parentheses denote the spurious eigenvalue.

Table 6 The former five modes for a confocal elliptical annulus.

Method \ Eigenmode	mode 1	mode 2	mode 3	mode 4	mode 5
Present method	 $k = 5.104$	 $k = 5.104$	 $k = 5.699$	 $k = 5.709$	 $k = 6.251$
Complex-valued BEM (No. elements=100)	 $k = 5.112$	 $k = 5.112$	 $k = 5.707$	 $k = 5.717$	 $k = 6.259$
ABQUAS (No. elements=2460)	 $k = 5.104$	 $k = 5.104$	 $k = 5.699$	 $k = 5.709$	 $k = 6.251$

## 零場邊界積分方程法於橢圓形薄膜之 真假根問題分析

李家瑋<sup>1</sup>、陳正宗<sup>1,2</sup>、呂學育<sup>3</sup>

<sup>1</sup>國立台灣海洋大學河海工程學系

<sup>2</sup>國立台灣海洋大學機械與機電工程學系

<sup>3</sup>中華科技大學航空機械系

M98520012@mail.ntou.edu.tw

**國科會計劃編號:**

**NSC 98-2221-E-019-017-MY3**

### 摘要

本文使用零場邊界積分方程法來探討使用邊界元素法求解橢圓形薄膜特徵值問題時所產生的真假根問題。為了能夠解析橢圓形邊界的特徵值問題，則需採用橢圓座標及 Mathieu 函數來分析。將基本解在橢圓座標下展開成退化核，邊界密度則使用特徵函數展開。Jacobian 項會存在於退化核、邊界密度和邊界積分裡，但會互相對消。因此正交關係在邊界積分裡是被保留的。有趣的是我們發現假若只使用實部或虛部核函數處理單連通的橢圓形薄膜，亦會有假根的產生。即使我們使用複數核函數，在共焦點的多連通橢圓薄膜也是有假根的產生。假根的產生是取決於內邊界的幾何形狀和所使用的方法。上述的兩個發現分別與圓形和同心圓環薄膜的結論是相同的。使用邊界元素法與有限元素法的套裝軟體 ABAQUS 所得數值結果亦驗證本文的正確性，且均可得到一致的結果。

**關鍵詞：**特徵解、零場邊界積分方程式、橢圓座標，Mathieu 函數，Jacobian，退化核。